

## Complex Metal Halide Oxides (2). Layered Complex Metal Chloride Oxides Having the X1X2 Structure as Catalysts for the Oxidative Dehydrogenation of Ethane

Sui Wen Lin, Young Chul Kim,<sup>†</sup> and Wataru Ueda\*

Department of Environmental Chemistry and Engineering, Tokyo Institute of Technology,  
4259 Nagatuta, Midori-ku, Yokohama 226

<sup>†</sup>Department of Material Chemical Engineering, Chonnam National University,  
300 Yongbong-dong, Buk-Gu, Kwangju 500-757, Korea

(Received December 26, 1997)

$\text{SrBi}_3\text{O}_4\text{Cl}_3$  with the X1X2 structure, in which metal–oxygen sheets were separated by single chlorine layers and double chlorine layers alternately, has been prepared and tested as a catalyst for the oxidative dehydrogenation of ethane.  $\text{SrBi}_3\text{O}_4\text{Cl}_3$  crystallized in space-group  $I4/mmm$  with lattice parameters of  $a = 3.9370(1)$ ,  $c = 27.0177(7)$  Å. The structure was refined by a Rietveld analysis, which showed that between two Bi(1) and Bi(2) sites, the former being of Bi in the metal–oxygen sheet faced the single chlorine sheet and the later faced the double chlorine sheet, strontium ions occupied the Bi(2) site only, and did not occupy the Bi(1) site. The  $\text{SrBi}_3\text{O}_4\text{Cl}_3$  catalyst showed a good catalytic performance for the oxidative dehydrogenation of ethane. Particularly, a high selectivity to ethene of more than 90% was obtained. Based upon an investigation of the potential role of chlorine during the course of the reaction, it was apparently shown that a role of surface chlorine species was important, rather than gas-phase chlorine, for the reaction. It is considered that the high selectivity to ethene can be attributed to the fact that the chlorine radical mechanism operates on the catalysts, and that the surface chlorine blocks the formation of active-oxygen species to prevent destructive oxidation reactions.

Bismuth chloride oxides have interesting properties leading to potential applications; luminescence and high-temperature superconductivity properties of this compound have been reported.<sup>1–3)</sup> In previous papers<sup>4–10)</sup> we demonstrated that layered complex metal chloride oxides based on bismuth have a good catalytic performance for the oxidative coupling of methane. A high selectivity to  $\text{C}_2$ -hydrocarbon was obtained. Particularly, the ratio of ethene to ethane was high; for example, with a  $\text{NaCa}_2\text{Bi}_3\text{O}_4\text{Cl}_6$  catalyst, a ethene-to-ethane ratio of 34.7 was observed at a methane conversion of 33.8%, and a total  $\text{C}_2$  selectivity of 43.2%. The result also revealed that the selectivity to ethene was sensitive to the state of chlorine in the bismuth chloride oxide catalysts, suggesting that the chloride ion in the structure is the key agent of hydrogen abstraction from methane for the production of methyl radicals.

Recently, we have tested various layered complex metal chloride oxides as catalysts for the oxidative dehydrogenation of ethane to ethene with molecular oxygen, and found that a  $\text{BiOCl}$  catalyst having X2 type structure (double chlorine sheet) showed high activity and selectivity in the oxidative dehydrogenation of ethane, but was rather unstable. On the other hand,  $\text{LiBi}_3\text{O}_4\text{Cl}_2$  catalyst having a single chlorine layer between metal–oxygen sheets (X1 type) displayed an extremely high durability for the reaction, but showed a moderate catalytic performance. It can therefore be expected that the X2-type phase could be stabilized by a structural

combination with a highly stable X1-type unit without diminishing the high activity of the X2-type catalyst. In this research, X1X2-type catalysts were synthesized and characterized structurally using the Rietveld method. The structure of the  $\text{SrBi}_3\text{O}_4\text{Cl}_3$  catalyst and its catalytic performance for the oxidative dehydrogenation of ethane are reported.

### Experimental

**Material Synthesis.**  $\text{MBi}_3\text{O}_4\text{Cl}_3$  (M: Sr, Pb) were synthesized by a solid state reaction of stoichiometric mixtures of bismuth oxide (99.99% pure), bismuth chloride oxide and strontium chloride (99%) or lead chloride at 700 °C in alumina crucibles for 20 h in air. X-Ray powder diffractometry ( $\text{Cu K}\alpha$  radiation) was used to ascertain the phase purity, to determine the sub-unit cell dimensions, and to investigate the phase change before and after the reaction. The  $\text{SrBi}_3\text{O}_4\text{Cl}_3$  sample used for the Rietveld analysis was prepared with excess strontium chloride (1.2-times of the stoichiometric amount) at 700 °C for 20 h, and was washed in an acetone–aqueous solution (80 vol%) in order to remove the excess of strontium chloride. The washed sample was dried at 50 °C for 4 h, then calcined at 900 °C for 5 h. Powder X-ray diffraction data for  $\text{SrBi}_3\text{O}_4\text{Cl}_3$  were collected using auto-monochromated  $\text{Cu K}\alpha$  radiation. Data suitable for a structure solution and refinement were collected over the range  $10^\circ < 2\theta < 100^\circ$  in  $0.04^\circ$  steps. A data analysis was carried out by the Rietveld method using the RIETAN program.<sup>11)</sup>

**Catalytic-Reaction Apparatus.** A catalytic reaction was carried out in a fixed-bed reactor at atmospheric pressure. The reactor was made of alumina tubing (11 mm o. d.), mounted horizontally in

a tubular furnace. The catalyst was placed at the center of the reactor and held in place by a piece of quartz wool. Two single-walled sealed alumina tubes (6 mm o.d.) were inserted from both sides of the reactor, which were used for reducing the empty space. One of the sealed ends, which was inserted into the catalyst zone, served as a thermo-well for measuring the reaction temperature, while the other was for supporting the catalyst in the reactor. The amount of catalyst used, unless indicated otherwise, was 4 g, which was diluted by quartz sand (catalyst : quartz sand = 1 : 1 (wt%)). The total flow rate was  $50 \text{ ml min}^{-1}$  (ethane : oxygen : nitrogen = 2 : 1 : 7), unless otherwise noted. It was confirmed that no reaction took place when the reaction was carried out without oxygen or a catalyst. The reaction products were separated with Porapak Q, T and Molecular sieve-13X, and were analyzed using a gas chromatograph equipped with a thermal-conductivity detector (TCD).  $\text{N}_2$  in the feed was used as an internal standard for calculating the conversion and selectivity. The conversion and selectivity were calculated based on the reacted ethane, and the carbon and oxygen balances were nearly 100%. At the reactor outlet, a water trap, cooled to  $0^\circ\text{C}$ , was used to remove the produced  $\text{H}_2\text{O}$  and a small amount of evolved hydrogen chloride from the exit gas stream. In order to understand the addition effect of gas-phase chlorine, hydrogen chloride gas was introduced to the reactant flow by a gas feeder. The evolved chlorine amount in the solution was measured periodically by a titration method.

## Results and Discussion

**Structure Determination.** The complex bismuth halide oxides were the parents of a whole family of phases with halogen sheet structures. Their principal structure characteristics, according to Sillén, are the presence of metal-oxygen sheets separated by halogen sheets.<sup>12)</sup> Large cations often occur in place of bismuth ions, and play the same structural role. A large number of metal oxides based on fluorite-like layers  $[\text{M}_2\text{O}_2]$  intergrew with single, double, or triple halide layers, forming  $/\text{M-O/X/M-O}/$ ,  $/\text{M-O/XX/M-O}/$  or  $/\text{M-O/XXX/M-O}/$  layered structures, such as  $\text{PbBiO}_2\text{Cl}$  (X1),  $\text{BiOCl}$  (X2), and  $\text{Ca}_{1.25}\text{Bi}_{1.5}\text{O}_2\text{Cl}_3$  (X3), respectively. More complex in-

tergrowths, such as X1X2, are also possible. Recently, an analogous phase containing "triple" fluorite layers,  $[\text{M}_3\text{O}_4]$ , has also been reported.<sup>13,14)</sup> The structure suggests the existence of a new family of layered metal halide oxides parallel with the well known Sillén phases,  $[\text{M}_2\text{O}_2]\text{X}_n$ .

In the present work, strontium ions were introduced in the place of bismuth ions of the metal-oxide sheets  $[\text{M}_2\text{O}_2]$ , and the resulting synthesized layered chloride oxide was  $\text{SrBi}_3\text{O}_4\text{Cl}_3$ . A preliminary analysis of the X-ray data for  $\text{SrBi}_3\text{O}_4\text{Cl}_3$  suggested that a layered structure was formed. The powder pattern of  $\text{SrBi}_3\text{O}_4\text{Cl}_3$  was indexed, and gave a primitive tetragonal cell with approximate dimensions of  $a=3.93$ ,  $c=27.02 \text{ \AA}$ . Since the reflection condition,  $hkl$ , was  $h+k+l=2n$ , and physical tests on the non-centro-symmetry were negative, the centrosymmetric space group  $I4/mmm$  was chosen, consistent with the results of the structure analysis. From the parameter of the cell and the characterization of the XRD pattern, the X1X2 structure was considered, in which the metal-oxygen sheets were separated by a single chloride layer and double chlorine layers, alternately. Further, this structure has finally been determined by the Rietveld method. The details are given in Table 1. Final Rietveld plots for the X-ray refinement are given in Fig. 1. The refinement proceeded straightforwardly, which allowed an anisotropic

Table 1. Crystal Data and Refinement

Crystal system	Tetragonal
Space group	$I4/mmm$
Cell parameters	$a = 3.9370(1) \text{ \AA}$ $c = 27.0177(7) \text{ \AA}$
$2\theta$ range	$10\text{--}100^\circ$ (Excluded regions in $29.0^\circ\text{--}31.0^\circ$ )
No. reflections	156
No. points	2250
$R_{\text{wp}}$ $R_{\text{p}}$	12.74%, 9.56%

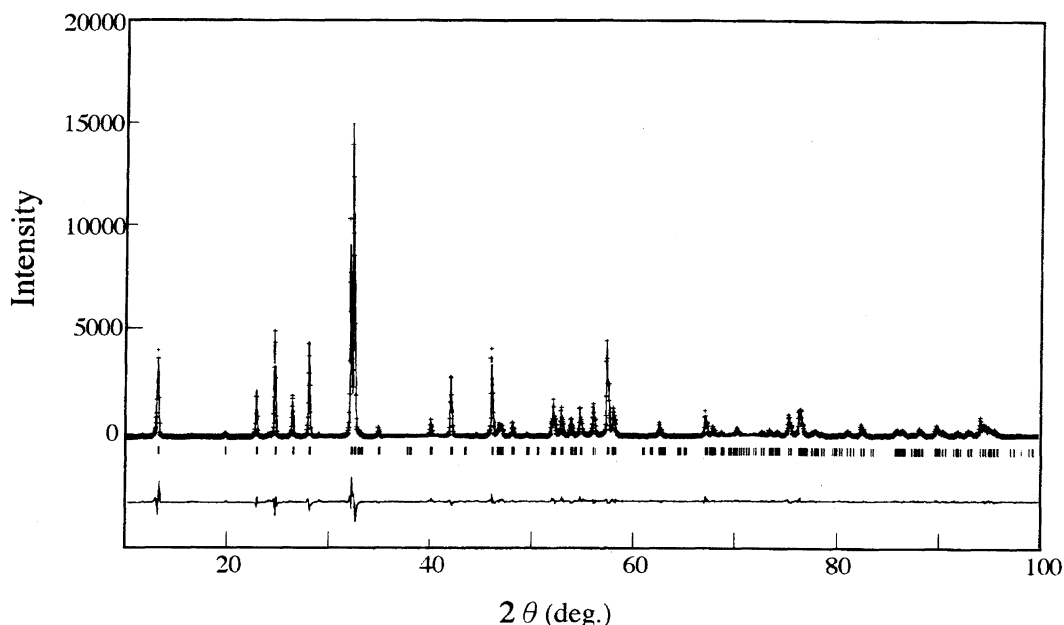


Fig. 1. Rietveld fit for  $\text{SrBi}_3\text{O}_4\text{Cl}_3$ , X-ray data.

temperature factor for the structural atoms. The final refined atomic parameter for  $\text{SrBi}_3\text{O}_4\text{Cl}_3$  are given in Table 2.

The structure is shown in Fig. 2, and the formula is  $\text{Cl/Bi-O-Bi(Sr)/Cl}_2\text{/Bi(Sr)-O-Bi/Cl}$ . It can be seen that a  $[\text{M}_2\text{O}_2]^{n+}$  ( $\text{M: Bi, Sr}$ ) layer is present. This cationic layer is balanced by the anionic chlorine layers. In the metal–oxygen layers oxygen was in tetrahedral coordination to metal ion M, while in the chloride layers chlorine was in 6-fold coordination. As a result, a square of four oxygens is located above the metal ions and a square of four chlorides below, as shown in Fig. 2. The double chlorine layers are combined by the Van der Waals bond. In general, strontium ions can occupy both the Bi(1) and Bi(2) sites in the metal–oxygen sheets by replacing bismuth ions with strontium ions. However, as indicated by the result of the structural analysis in Table 2, it has been revealed that the strontium ion occupies only the Bi(2) site,

Table 2. Final Atomic Parameters for  $\text{SrBi}_3\text{O}_4\text{Cl}_3$

Atom	Site	Occupancy	x	y	z
Bi(1)	4e	1.0	0	0	0.0721(2)
Bi(2)	4e	0.5	0	0	0.3447(4)
Sr(1)	4e	0.5	0	0	0.3276(8)
O(1)	8g	1.0	0.5	0	0.107(1)
Cl(1)	4e	1.0	0	0	0.205(1)
Cl(1)	2b	1.0	0	0	0.5

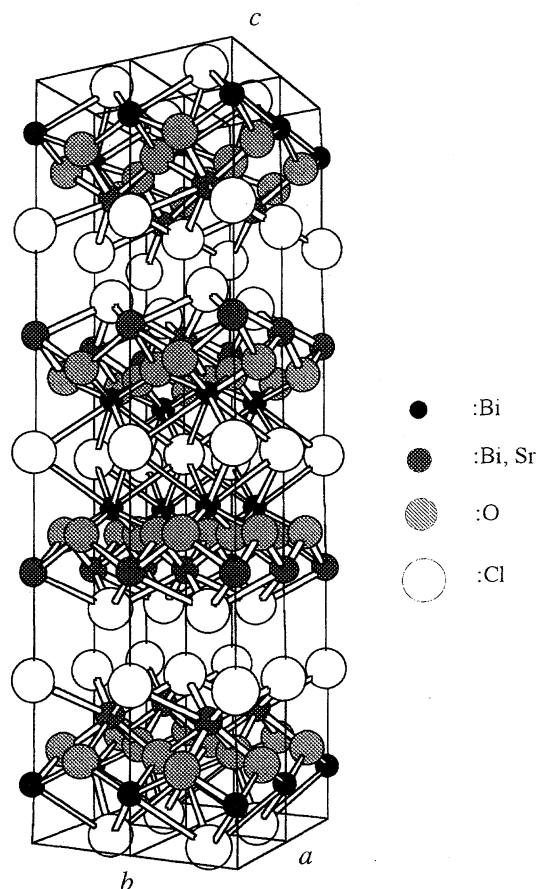


Fig. 2. The structure of  $\text{SrBi}_3\text{O}_4\text{Cl}_3$  along [010].

and the space coordinate of the strontium atom shifts to (0, 0, 0.3276) from the Bi(2) site (0, 0, 0.3447). Because the shift is less, the metal–oxygen sheets have no obvious distortion, and can keep the symmetry of the layered structure.

Comparing the details of the Bi–Cl and Sr–Cl distances of the  $\text{SrBi}_3\text{O}_4\text{Cl}_3$  compound, the Bi(1)–Cl bond length is longer than the Bi(2)–Cl bond length (Bi(1)–Cl = 3.4 Å, Bi(2)–Cl = 3.0 Å). This can be attributed to the difference of the electron environment between two bismuth ions because of the selective replacement of a bismuth ion by a strontium ion. The bond length of Sr–Cl was 2.9 Å, which is similar to that of Bi(2)–Cl. For the fundamental phase of  $\text{BiOCl}$ ,<sup>15</sup> which has an X2-type structure, the Bi–Cl bond length is reported to be 3.05 Å. On the other hand, in the case of the  $\text{SrBiO}_2\text{Cl}$  phase,<sup>16</sup> which is a distorted variant of the Sillén X1 structure, the corresponding bond lengths in  $\text{SrBiO}_2\text{Cl}$  are longer than the  $\text{BiOCl}$  (X2); the Bi–Cl distances of  $\text{SrBiO}_2\text{Cl}$  are 3.49–3.53 Å. In the structures of the phases referred to above, the metal atom is surrounded by four oxygen neighbors and by four nearest chlorines. The  $\text{Bi}_2\text{O}_2$  layers are crystallographically identical.<sup>15</sup> The difference is the chlorine layer. The shorter bond length of the Bi–Cl in  $\text{BiOCl}$  structure can be attributed to the existence of double chlorine layers between the metal–oxygen sheets. By a repelling effect between the chlorine atoms in the double chlorine layers, the chlorine ions become close to the metal ions, so that the bond length of Bi–Cl in  $\text{BiOCl}$  becomes shorter than that in  $\text{SrBiO}_2\text{Cl}$  (X1). It is also considered for the same reason as above that the Bi(1)–Cl bond length is longer than the Bi(2)–Cl bond length in the  $\text{SrBi}_3\text{O}_4\text{Cl}_3$  structure. In general, the  $\text{M}_2\text{O}_2$  layers are probably regular when the cations M are identical, or when their positions are occupied randomly by replaced atoms of different kinds. However, a partial deformation with a consequent lowering of the symmetry of the unit is possible. In the structure of  $\text{SrBi}_3\text{O}_4\text{Cl}_3$ , we found that the space coordinate of the replaced strontium ion had a smaller shift from the Bi(2) site. This can be attributed to a space hinder, once because the ion radius of strontium is bigger than that of the bismuth ion. As pointed out in Fig. 3, the  $\text{Sr}_2\text{Bi}_3\text{O}_4\text{Cl}_5$  and  $\text{Sr}_3\text{Bi}_3\text{O}_4\text{Cl}_7$  catalysts have no variation in the structural parameters, even though the amount of strontium chloride was increased in the synthesitic stage. The same X1X2-type structure and unit-cell parameters have been observed with increasing the amount of strontium chloride; instead of that excess, the strontium chloride phase was observed in the XRD pattern. It is clear that catalysts having a composition of  $\text{Sr}_2\text{Bi}_3\text{O}_4\text{Cl}_5$  and  $\text{Sr}_3\text{Bi}_3\text{O}_4\text{Cl}_7$  are based on the structure of  $\text{SrBi}_3\text{O}_4\text{Cl}_3$ .

**Catalytic Performances of  $\text{SrBi}_3\text{O}_4\text{Cl}_3$  and  $\text{PbBi}_3\text{O}_4\text{Cl}_3$ .** We tested  $\text{MBi}_3\text{O}_4\text{Cl}_3$  (M: Pb, Sr) catalysts having the X1X2-type structure for the oxidative dehydrogenation of ethane. The synthesized  $\text{SrBi}_3\text{O}_4\text{Cl}_3$  and  $\text{PbBi}_3\text{O}_4\text{Cl}_3$  samples have the same structure (X1X2 type), which was determined by X-ray diffractometry. The catalytic performances of two samples are shown in Fig. 4. Both of the two samples showed a good catalytic performance for the formation of ethene; the  $\text{SrBi}_3\text{O}_4\text{Cl}_3$  catalyst gave 89% selectivity

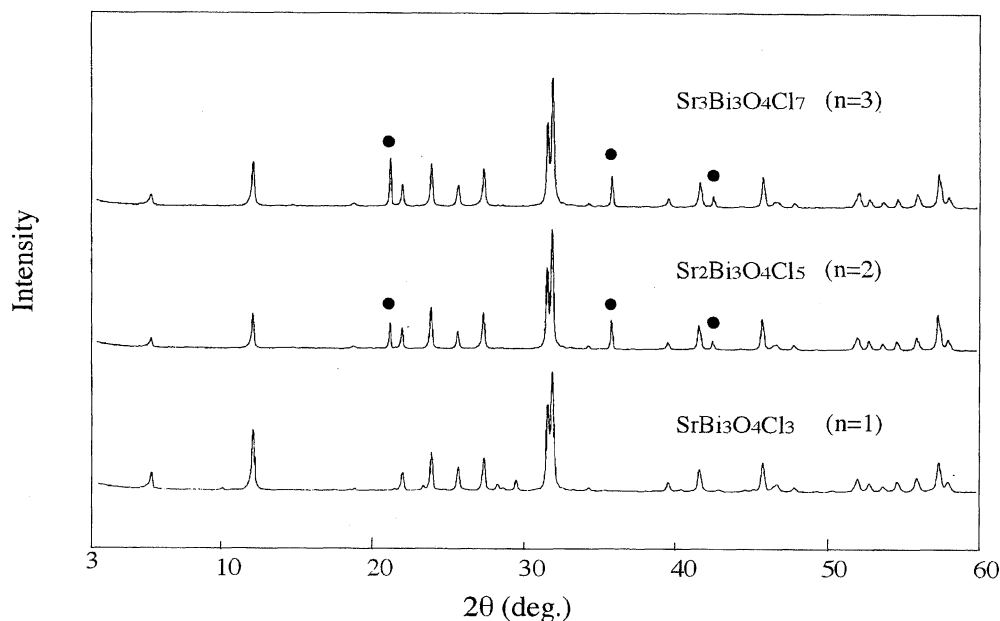


Fig. 3. The XRD pattern of  $\text{Sr}_n\text{Bi}_3\text{O}_4\text{Cl}_{2n+1}$  (●:  $\text{SrCl}_2$  phase).

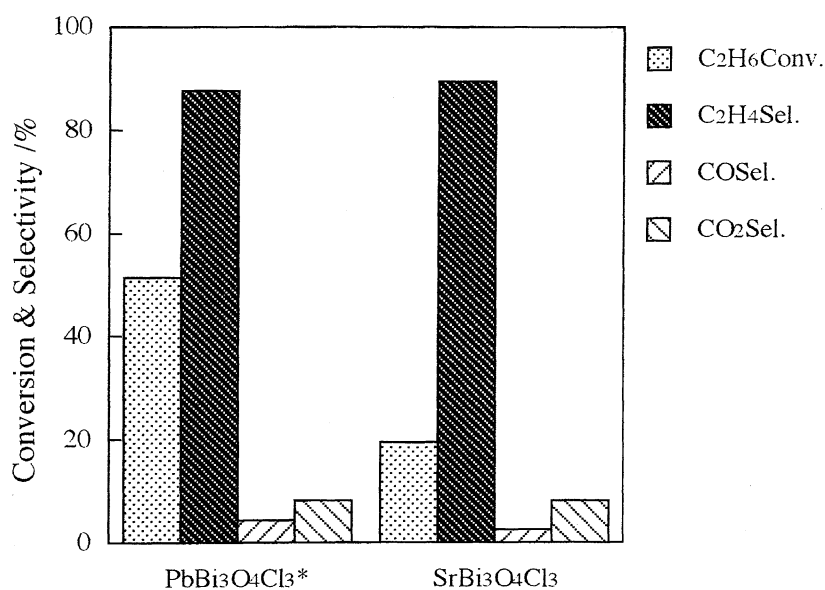


Fig. 4. The catalytic performance of  $\text{PbBi}_3\text{O}_4\text{Cl}_3$  and  $\text{SrBi}_3\text{O}_4\text{Cl}_3$  catalysts in the oxidative dehydrogenation of ethane. (Data were collected after 6 h reaction, \* data was collected after 1 h reaction).

to ethene, and 87% selectivity to ethene was obtained over the  $\text{PbBi}_3\text{O}_4\text{Cl}_3$  catalyst. In spite of the same structure, the  $\text{PbBi}_3\text{O}_4\text{Cl}_3$  catalyst showed a higher activity for the conversion of ethane than the  $\text{SrBi}_3\text{O}_4\text{Cl}_3$  catalyst. However, since the  $\text{PbBi}_3\text{O}_4\text{Cl}_3$  catalyst was unstable under the reaction condition, the activity decreased readily accompanying a structural decomposition within a short reaction period. This can be simply attributed to a fault of the thermal stability of  $\text{PbBi}_3\text{O}_4\text{Cl}_3$ . On the other hand, the  $\text{SrBi}_3\text{O}_4\text{Cl}_3$  catalyst exhibited a good structural stability; there was no detectable change in the structure of the catalyst before and after the reaction.

Although one may think that the high selectivity to ethene

over the  $\text{SrBi}_3\text{O}_4\text{Cl}_3$  catalyst can be imputed to the lower ethane conversion (19%), we consider that it is not a simple effect of the overall conversion, and that the selectivity to ethene is controlled by the structure of layered complex chloride oxide catalysts. The reason is as follows: The  $\text{SrBi}_3\text{O}_4\text{Cl}_3$  catalyst was calcined at 700 °C for 20 h. Therefore, the catalyst was well-sintered and its surface area was less than  $1 \text{ m}^2 \text{ g}^{-1}$ , so that it inevitably showed a lower activity for the oxidative dehydrogenation of ethane. On the other hand, the  $\text{Sr}_2\text{Bi}_3\text{O}_4\text{Cl}_5$  and  $\text{Sr}_3\text{Bi}_3\text{O}_4\text{Cl}_7$  catalysts [ $\text{Sr}_n\text{Bi}_3\text{O}_4\text{Cl}_{2n+1}$  ( $n=1, 2, 3$ )], based on the  $\text{SrBi}_3\text{O}_4\text{Cl}_3$  structure with excess  $\text{SrCl}_2$  phase, showed a higher ethane conversion. For example, when  $n=3$ , the ethane conversion

increased from 19.5% ( $n=1$ ) to 43.8%, and the selectivity to ethene remained at 89%. Since the  $\text{SrCl}_2$  phase is inactive for the oxidative dehydrogenation of ethane, it can be considered that the presence of excess  $\text{SrCl}_2$  results in the formation of smaller crystalline particles of  $\text{SrBi}_3\text{O}_4\text{Cl}_3$ , thus increasing the amount of the active phase in which the (010) plane is believed to be responsible for the selective oxidative dehydrogenation of ethane. Moreover, it can be expected that an excess addition of  $\text{SrCl}_2$  can minimize the formation of other phase impurities or amorphous metal oxide, which might cause lower selectivities in the catalytic reaction. As a consequence, the X1X2-type structure is responsible for the high selectivity to ethene, even at a high conversion of ethane in the oxidative dehydrogenation of ethane.

Recently, we found that catalysts containing strontium as an alkaline-earth constituent and potassium as an alkali constituent were highly active and selective for the oxidative dehydrogenation of ethane.<sup>17)</sup> Particularly, the  $\text{KSr}_2\text{Bi}_3\text{O}_4\text{Cl}_6$  catalyst, having the X1X2 structure, showed an extremely high selectivity, more than 90%, even under a high-oxygen partial pressure condition and at high molar ratios of oxygen to ethane, and gave 70% yield of ethene at 640 °C under an optimized feed gas composition. The high selectivity at high ethane conversion is the characteristic feature of this catalyst system compared to other halogen-free oxide catalyst systems.<sup>18–21)</sup>

It has been found that a substantial amount of ethene was obtained over the chlorine-contained catalysts in the oxidative coupling of methane, while with oxide catalysts the major  $\text{C}_2$  product was usually ethane. Moreover, catalysts based on bismuth chloride oxide showed a high selectivity for the oxidative dehydrogenation of ethane. These results simply suggest that chlorine is a key element in the C–H bond activation of ethane to ethene. Since the bismuth chloride oxide-based catalyst loses a small amount of chlorine under the reaction condition, and also that the chlorine atoms are known to serve as chain carriers in the homogeneous dehydrogenation of ethane, chlorine may be involved in a purely surface catalysis, in a gas-phase interaction, or in some combination of both. Ahmed and Moffat suggested that the gas-phase chlorine may play a role in the oxidative dehydrogenation of ethane.<sup>22)</sup> However, Conway and Lunsford have shown that there is no correlation between the rate of chlorine loss from a  $\text{Li}^+-\text{MgO}-\text{Cl}^-$  catalyst and its activity.<sup>23)</sup>

We investigated this problem. The bismuth chloride oxide catalyst release hydrogen chloride in the oxidative dehydrogenation of ethane, as shown in Table 3, where the loss of chlorine from the catalyst in the integral reactor as a function of time on stream is summarized. If the chlorine radicals are produced in the gas phase along with the dissociation of hydrogen chloride under a high reaction temperature, and the subsequent reaction of the chlorine radical occurs with ethane, the loss of chlorine may be attributed largely to the rate of ethane oxidation. However, as indicated in Table 3, there was no correlation between the rate of chlorine evolution from the catalyst and the conversion of ethane. For example, the rate of chlorine loss decreased from the  $8.48 \mu\text{mol h}^{-1}$  to  $5.37$

Table 3. Conversion of Ethane and Evolution of Hydrogen Chloride over  $\text{SrBi}_3\text{O}_4\text{Cl}_3$

Time on stream (h)	Conversion <sup>a)</sup> (%)	Cl evolution <sup>b)</sup> ( $\mu\text{mol h}^{-1}$ )	$\text{C}_2\text{H}_4/\text{Cl}^{\text{c)}$ (Atomic ratio)
1	19.9	8.48	569
2	21.3	6.78	757
3	19.5	5.65	927

a) Reaction condition: reaction temperature: 660 °C, catalyst weight: 4 g, total flow rate:  $50 \text{ ml min}^{-1}$  ( $\text{C}_2\text{H}_6 : \text{O}_2 : \text{N}_2 = 2 : 1 : 7$ ).

b) The lost amount of chlorine as hydrogen chloride from the  $\text{SrBi}_3\text{O}_4\text{Cl}_3$  catalyst. c) The molecules of ethene formed per molecule of chlorine released from the  $\text{SrBi}_3\text{O}_4\text{Cl}_3$  catalyst.

$\mu\text{mol h}^{-1}$  over a period of 3 h under the reaction condition, whereas the ethane conversion showed no obvious change. Moreover, the integrated  $\text{C}_2\text{H}_4/\text{Cl}$  ratio (the molecules of ethene formed per molecule of chlorine released from the catalyst) ranged from 569 to 927. The addition effect of hydrogen chloride gas in the reactant gas was also investigated. The results are shown in Fig. 5. The oxidation of ethane was first conducted over the  $\text{SrBi}_3\text{O}_4\text{Cl}_3$  catalyst; after a 6 h reaction hydrogen chloride gas ( $20 \mu\text{mol h}^{-1}$ ) was introduced to the reactant flow. It was found that the conversion and selectivity revealed no obvious changes. This result further supports the role of gas-phase chlorine, even if it exists, is very small in the oxidative dehydrogenation of ethane over the  $\text{SrBi}_3\text{O}_4\text{Cl}_3$  catalyst. On the other hand, the activity decrease along with the loss of chlorine was restrained by the addition of hydrogen chloride gas. We suggest that the role of a surface-active chlorine species is important rather

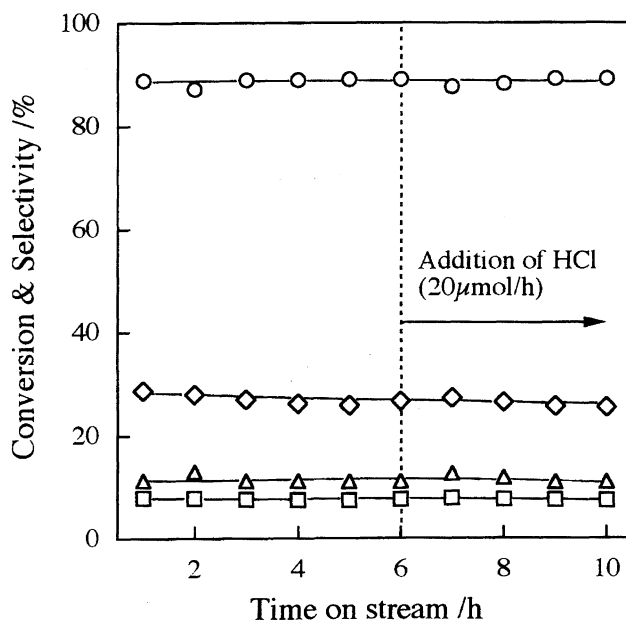


Fig. 5. The oxidative dehydrogenation of ethane as a function of time on stream over  $\text{SrBi}_3\text{O}_4\text{Cl}_3$  catalyst. Reaction temperature 640 °C, catalyst weight 2 g, total flow rate  $50 \text{ ml min}^{-1}$  ( $\text{C}_2\text{H}_6 : \text{O}_2 : \text{N}_2 = 1 : 4 : 15$ ). The feed of  $\text{HCl}$  ( $20 \mu\text{mol h}^{-1}$ ) started at the time indicated by the dotted line. ( $\diamond$ :  $\text{C}_2\text{H}_6$  Conv.  $\square$ :  $\text{O}_2$  Conv.  $\circ$ :  $\text{C}_2\text{H}_4$  Sel.  $\triangle$ :  $\text{CO}_x$  Sel.)

than gas-phase chlorine in the oxidative dehydrogenation of ethane over the layered complex metal chloride oxides.

It appears that the oxidative dehydrogenation of ethane occurs through a direct interaction with the chloride-containing surface of the bismuth chloride oxide-based catalysts. It can be considered that the lattice chloride ion releases electrons to the metal-oxygen sheets to be a radical chlorine by a thermal process; thus, the radical chlorine formed would be capable for activating ethane to ethyl radicals. The ethyl radicals immediately convert into ethene. The abstracted hydrogens from ethane are oxidized over the metal-oxygen sheets by molecular oxygen at the second reaction step, and finally the catalytic cycle is completed. The characteristics of the  $\text{SrBi}_3\text{O}_4\text{Cl}_3$  catalyst are a high selectivity to ethene and a low activity for a destructive reaction, as shown in Fig. 4. It therefore seemed that another important role of the surface chlorine is to block sites at which very reactive oxygen species may be formed.

**Conclusion.** The  $\text{SrBi}_3\text{O}_4\text{Cl}_3$  catalyst has been synthesized, and its proposed X1X2 structure was proved and refined by a Rietveld analysis. It was found that in the refined structure of  $\text{SrBi}_3\text{O}_4\text{Cl}_3$ , the strontium ion occupied only the Bi(2) site, and had a smaller shift in the space coordinate. A catalyst having this X1X2 structure showed a good catalytic performance for the oxidative dehydrogenation of ethane. The results indicated that the reaction occurs through a direct interaction with the chloride-containing surface of the X1X2-type catalysts, rather than a homogenous reaction. It is considered that the high selectivity to ethene can be attributed to the surface chloride radical mechanism, and that the surface chlorine blocks the active site which may provide active oxygen species for destructive oxidation.

This work has been carried out partly as a research project of the Japan Petroleum Institute commissioned by the Petroleum Energy Center with the support of the Ministry of International Trade and Industry.

## References

- 1) G. Blasse, J. Sytsma, and L. H. Brixner, *Chem. Phys. Lett.*, **155**, 64 (1989).
- 2) M. Al-Mamouri, P. P. Edwards, C. Greaves, and M. Slaski, *Nature (London)*, **369**, 382 (1994).
- 3) Z. Hiroi, N. Kobayashi, and M. Takano, *Nature (London)*, **371**, 139 (1994).
- 4) W. Ueda and J. M. Thomas, "Proc. 9th Int. Congr. Catal.," ed by J. M. Philips and M. Ternan, Chem. Inst. of Canada, Ottawa (1988), Vol. 2, p. 960.
- 5) W. Ueda and J. M. Thomas, *J. Chem. Soc., Chem. Commun.*, **1988**, 1148.
- 6) J. M. Thomas, W. Ueda, J. Williams, and K. D. M. Harris, *Faraday Discuss. Chem. Soc.*, **87**, 212 (1989).
- 7) W. Ueda, F. Sakyu, T. Isozaki, Y. Morikawa, and J. M. Thomas, *Catal. Lett.*, **10**, 83 (1991).
- 8) W. Ueda, T. Isozaki, Y. Morikawa, and J. M. Thomas, *Chem. Lett.*, **1989**, 2103.
- 9) W. Ueda, T. Isozaki, F. Sakyu, S. Nishiyama, and Y. Morikawa, *Bull. Chem. Soc. Jpn.*, **69**, 485 (1996).
- 10) R. Burch, S. Chalker, J. M. Thomas, W. Ueda, and P. Loader, *Appl. Catal.*, **82**, 77 (1992).
- 11) Y. I. Kim and F. Izumi, *J. Ceram. Soc. Jpn.*, **102**, 401 (1994).
- 12) L. G. Sillén, *Z. Anorg. Allg. Chem.*, **242**, 41 (1939); **246**, 115 (1941); **246**, 331 (1941).
- 13) B. Aurivillius, *Chem. Scripta*, **24**, 125 (1984).
- 14) C. J. Milne, P. Lightfoot, J. D. Jorgensen, and S. Short, *J. Mater. Chem.*, **5**, 1419 (1995).
- 15) L. G. Sillén, *Naturwissenschaften*, **22**, 318 (1942).
- 16) S. M. Fray, C. J. Milne, and P. Lightfoot, *J. Solid State Chem.*, **128**, 115 (1997).
- 17) W. Ueda, S. W. Lin, and I. Tohmoto, *Catal. Lett.*, **44**, 241 (1997).
- 18) E. Morales and J. H. Lunsford, *J. Catal.*, **118**, 225 (1989).
- 19) L. Ji and Liu, *Chem. Commun.*, **1996**, 1203.
- 20) E. A. Mamedov and V. C. Corberan, *Appl. Catal. A*, **127**, 1 (1995).
- 21) R. X. Valenzuela, J. L. G. Fierro, V. C. Corberan, and E. A. Mamedov, *Catal. Lett.*, **40**, 223 (1996).
- 22) S. Ahmed and J. B. Moffatt, *Appl. Catal.*, **58**, 83 (1990).
- 23) S. J. Conway and J. H. Lunsford, *J. Catal.*, **131**, 513 (1991).